Inorganic Chemistry

ARTICLE

pubs.acs.org/IC

New Types of Multishell Nanoclusters with a Frank−Kasper Polyhedral Core in Intermetallics

Vladislav A. Blatov,*[,†] Gregory D. Ilyushin,[‡] and Davide M. Proserpio[§]

[†]Samara State University, Ac. Pavlov St. 1, Samara 443011, Russia

[‡]Institute of Crystallography of RAS, Leninskii Prospekt 59, Moscow 117333, Russia

[§]Università degli Studi di Milano, Dipartimento di Chimica Strutturale e Stereochimica Inorganica (DCSSI), Via G. Venezian 21, 20133 Milano, Italy

Supporting Information

ABSTRACT: A comprehensive study of the occurrence of two-shell clusters with the first shell as a Frank−Kasper polyhedron Z12, Z14, Z15, or Z16 (Frank−Kasper nanoclusters) is performed for 22 951 crystal structures of intermetallics containing only metal atoms. It is shown that besides the familiar Bergman and Mackay clusters, two more types of high-symmetrical icosahedron-based nanoclusters are rather frequent; they both have a 50-atom second shell. Moreover, two types of high-symmetrical Frank−Kasper nanoclusters with a Friauf-polyhedron (Z16) core are revealed; these nanoclusters have 44 and 58 atoms in the second shell. On the contrary, Z14 and Z15 Frank−Kasper polyhedra have been found to be rare and improper to form distinct nanoclusters in crystals. The second shells of Frank−Kasper nanoclusters have been revealed possessing their own stability: they can be realized in nanoclusters with different internal polyhedra and can shift around the core shell. The role of Frank−Kasper nanoclusters in assembling intermetallic crystal structures is illustrated by several examples.

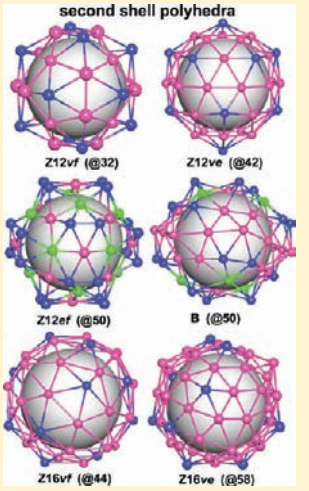

INTRODUCTION

In the structural chemistry of intermetallic compounds, the polyhedral models are widespread, where the crystal structure is perceived as an ensemble of clusters based on convex polyhedra. Since one of the most abundant coordination polyhedra in intermetallics is icosahedron, there is a known family of metal clusters with the icosahedral core. Two clusters of this family were described long ago by Mackay[1] and Bergman[2] and became of particular interest as structural units of quasicrystals.[3,4] Both types of clusters are two shell, i.e., the internal icosahedron (that can be centered or empty) is sheathed with a 42- or 32-atom shell, respectively. In the Mackay cluster the atoms of the outer shell are allocated above all 12 vertices and the centers of all 30 edges of the inner icosahedron (12 + 30 = 42), while in the Bergman cluster they are projected to the icosahedron vertices and the centers of all 20 faces (12 + 20 = 32). We emphasize that the Mackay cluster was initially derived theoretically[1] by considering maximal density packings of equal balls on the icosahedron surface; it was shown that the number of balls could not exceed 42. Thus, numbers 12, 42, 92, ... (in general $10n^2 + 2$) are "magic" for multishell clusters consisting of equal atoms. At the same time, packing of balls of different size can be characterized by other "magic" numbers that can result in discovering new clusters to be important for understanding the mechanisms of transformation of nanoparticles to periodic or aperiodic phases.

At present, the methods of modeling metal clusters are well developed and provide vast data on stable configurations of multicomponent atomic groups.[5,6] A crucial point is to check the results of modeling experimentally to prove if the cluster particles exist and participate in forming crystal structures. Direct methods like HREM are not precise enough to recognize in detail the structure of such small particles and to look into their outer shells. Diffraction methods require clusters to be incorporated into a bulky periodic crystal, but in this case, the immediate correlation with the results of modeling is lost because all model clusters are refined as finite objects. Nonetheless, Mackay and Bergman clusters were found in crystal structures, which proves the existence of locally stable ensembles in the macrophase.

Thus, one can consider the occurrence of a model cluster in crystal structures as good evidence of its stability and reality of existence, however not as a strict proof.[7] Besides, the abundance of a cluster in different intermetallics would prove the significance of such configuration for crystal formation processes at the

Received: March 10, 2011
Published: May 24, 2011

nanolevel. However, until recently there were no tools to search for large atomic fragments in about 30 000 three-periodic intermetallic frameworks, the crystallographic data on which are stored in Pearson's Crystal Data (PCD), ICSD, and CRYSTMET electronic databases.

Recently,[8] we developed a computer procedure for fast automated searching for cluster fragments of any complexity in crystal structures of any nature. This procedure was implemented into the program package TOPOS,[9] which provides processing large crystallographic databases. As a result, the tools appeared for a guided search for metal clusters through the whole set of crystallographic information.

Using these tools we have shown that many complicated intermetallics can be uniformly represented as ensembles of multishell clusters (onion-like structure) of a nanosize (>1 nm), which we call *nanoclusters*. In particular, we found that $NaCd_2$ and β-Mg_2Al_3 (so-called Samson's phases)[10−13] can be constructed with two types of two-shell nanoclusters, 61-atom (1@16@44) nanocluster A and 63-atom (1@12@50) nanocluster B whose inner shell is the 16-atom Friauf polyhedron (one of Frank−Kasper polyhedra, Figure 1)[14] and icosahedron, respectively.[15,16] In the low-temperature phase β'-Mg_2Al_3 nanocluster B is preserved, and the structure transformation $\beta \rightarrow \beta'$ can be described in terms of slight reorganization of nanocluster A: it is split into two nanoclusters A1 (1@16@43) and A2 (1@15@41); the last one is based on another Frank−Kasper polyhedron, Z15 (Figure 1). Nanocluster B was found to be typical for intermetallics; it occurs in crystal structures of 44 Pearson classes including three Laves phases $MgCu_2$, $MgZn_2$, and $MgNi_2$, whereas nanocluster A is quite rare (it was revealed only in three Pearson classes). The number of atoms in the outer shell of the nanocluster B (50) is accidentally equal to the sum of the numbers of edges and faces of icosahedron (30 + 20 = 50), but not all edges of the inner icosahedron are centered in the projection by the atoms of the outer shell. In fact, 32 of the

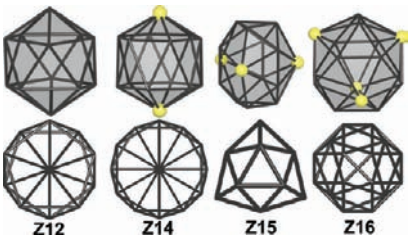

Figure 1. Frank−Kasper polyhedra Z12 (icosahedron, I_h), Z14 (D_{6d}), Z15 (D_{3h}), and Z16 (Friauf polyhedron, T_d) as well as their projections along the main symmetry axes (see Table 1 for details). The yellow balls correspond to 6-coordinated vertices.

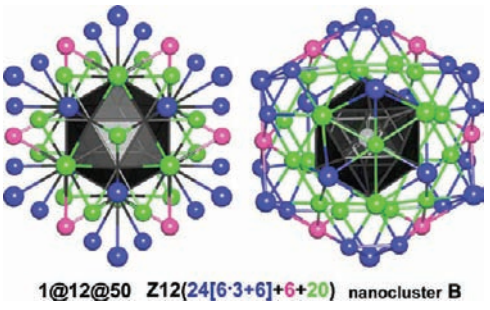

Figure 2. 1@12@50-atom nanocluster B [Z12(24[6·3 + 6] + 6 + 20)]: (left) a projection along the symmetry axis C_3 (the links between atoms of different shells are shown only); (right) a general view of the nested shells (links between atoms of different shells are not shown). The inner icosahedron (the first shell) is shown in black; the 50 atoms of the outer (second) shell which are projected to vertices, centers of edges, or faces of the icosahedron are colored in blue (24), magenta (6), or green (20), respectively.

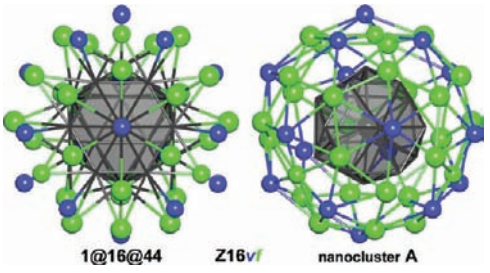

Figure 3. 1@16@44-atom nanocluster A Z16*vf*: (left) a projection along the symmetry axis C_3; (right) a general view of the nested shells. The inner Friauf Z16 polyhedron is shown in black; the 44 atoms of the outer shel, which are projected to all vertices or centers of faces of the Friauf polyhedron are colored in blue (16) or green (28), respectively.

Table 2. Second Shells in Z12-Based Nanoclusters 1@12@*N* with an Atom in the Center[a]

number of atoms (*N*)	number of structures		
1@12@*N*	D_{3d} symmetry	T_h symmetry	total
32	3[b]	202 (30[b])	205 (33[b])
36	4	9	13
42	82 (80[c])	11[c]	93 (91[c])
44	34	109	143
48		7	7
50	2316 (2293[d])	374[e]	2690
54	10		10
56	9	44	53
60	1		1
62	2		2

[a] Hereafter the "magic" numbers corresponding to the *vf*, *ve*, *ef*, or *vef* types of the second shell are in bold. [b] Z12*vf* Bergman type. [c] Z12*ve* Mackay type. [d] Nanocluster B Z12(24[6·3 + 6] + 6 + 20). [e] Z12*ef* type.

Table 1. Parameters of Frank−Kasper Polyhedra

polyhedron	*v*	*e*	*f*	symmetry	*v* + *f*	*v* + *e*	*e* + *f*	*v* + *e* + *f*
Z12 (icosahedron)	12	30	20	I_h (T_h, D_{3d})	32	42	50	62
Z14	14	36	24	D_{6d} (C_{6v} D_{3d})	38	50	60	74
Z15	15	39	26	D_{3h}	41	54	65	80
Z16 (Friauf polyhedron)	16	42	28	T_d	44	58	70	86

dx.doi.org/10.1021/ic2005024 |*Inorg. Chem.* 2011, 50, 5714–5724

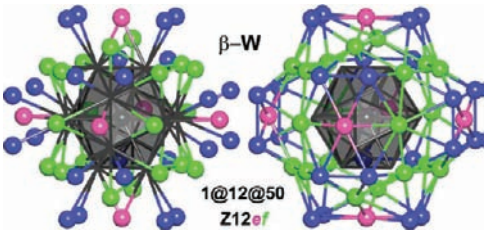

Figure 4. 1@12@50-atom nanoclusters Z12*ef* of T_h symmetry in the β-W: (left) links between atoms of different shells are shown only; (right) nested shells. The inner icosahedron is shown in black; the atoms of the outer shell which are projected to the centers of edges or faces of the icosahedron are colored in magenta or green, respectively.

Table 3. Second Shells in Z14-Based Nanoclusters 1@14@N with an Atom in the Center

number of atoms (N)	number of structures		
1@14@N	D_3 symmetry	C_{6v} symmetry	total
44		10	10
47	270		270
50	45	9	54
56	2	146	148
59	1		1

50 atoms are arranged as in the Bergman-type cluster (12 vertices +20 faces), whereas the other 18 atoms are allocated above the edges of the inner icosahedron forming a zone (Figure 2). The maximal point symmetry of the nanocluster is D_{3d} ($\bar{3}m$), which is preserved in the $NaCd_2$ and β-Mg_2Al_3 crystal structures.

The results described above raise two questions about possible forms of nanoclusters based on a Frank–Kasper polyhedral core. First, does the isomeric 63-atom nanocluster exist where the atoms of the outer shell are projected to the edges and faces of the core icosahedron? This Z12*ef* nanocluster would naturally complement the group of two-shell nanoclusters with icosahedral symmetry (I_h) along with 45-atom (1 + 12 + 32 = 45) Z12*vf* Bergman and 55-atom (1 + 12 + 42 = 55) Z12*ve* Mackay clusters. Hereafter we use the short ZXX*vef* notation for the two-shell nanoclusters where *all* vertices (*v*), edges (*e*), or faces (*f*) of the core ZXX Frank–Kasper polyhedron correspond to atoms of the outer shell and vice versa. To define the general type of the second shell of nanoclusters, where *v*, *e*, and *f* atoms are projected to vertices, edges, or faces of the core Frank–Kasper polyhedron, we use the signature ($v + e + f$). Owing to geometrical distortions, the projection could not coincide with the vertices, centers of edges, or faces but the displacements were visually insignificant. Nonetheless, to be independent of any geometrical distortion we use a topological criterion: an atom of the second shell is of the "*v*", "*e*", or "*f*" type if it is connected to one, two, or three atoms of the core polyhedron. For example, cluster B (Figure 2) can be denoted as Z12(24[6·3 + 6] + 6 + 20), where

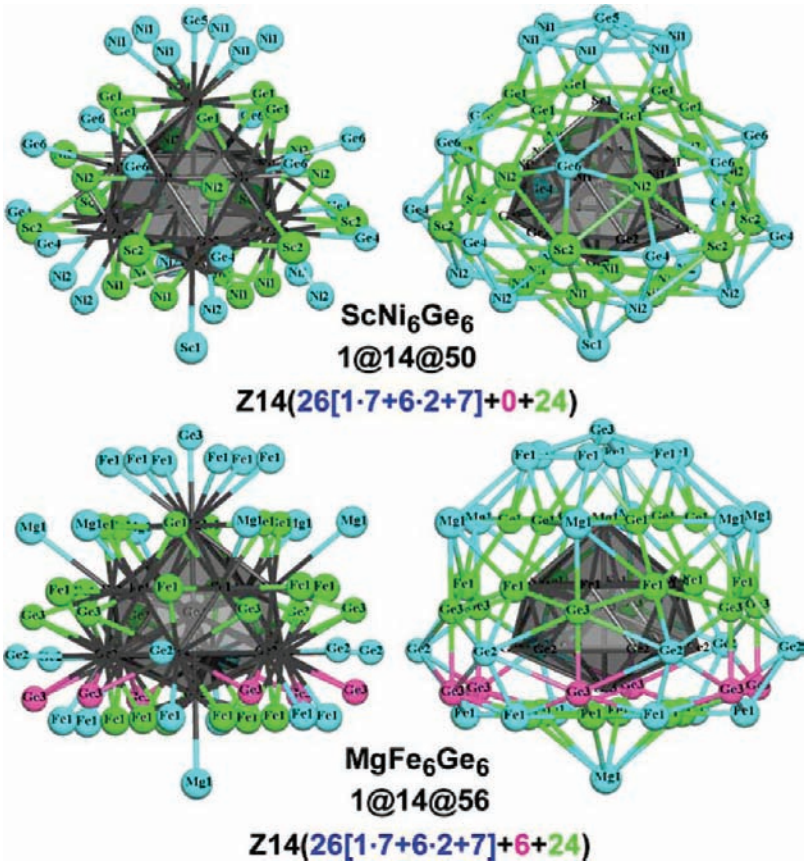

Figure 5. (Top) 1@14@50-atom nanocluster in the $ScNi_6Ge_6$ crystal structure Z14(26[1·7 + 6·2 + 7] + 0 + 24), and (bottom) 1@14@56-atom nanocluster in the $MgFe_6Ge_6$ crystal structure Z14(26[1·7 + 6·2 + 7] + 6 + 24). The symmetry of the nanoclusters is C_{6v}; the C_6 axis is vertical. The inner Z14 polyhedron is shown in black; the atoms of the outer shell which are connected to vertices, edges, or faces of the Z14 polyhedron are colored in cyan, magenta, or green, respectively.

dx.doi.org/10.1021/ic2005024 |*Inorg. Chem.* 2011, 50, 5714–5724

the detailed expression [6·3 + 6] shows that out of 24 "*v*" atoms 6 atoms are connected to different vertices of the core icosahedron while the remaining 18 atoms are arranged into triples connected to the same icosahedron vertices.

Another question arises when considering the 61-atom nanocluster A (Figure 3). This nanocluster keeps the maximal tetrahedral symmetry T_d ($\bar{4}3m$) of its core, the Z16 Friauf polyhedron, because the 44 atoms of the second shell are allocated above all 16 vertices and 28 faces of Z16. In this relation nanocluster A can be considered as a topological analog of the Bergman cluster based on another polyhedral core but having the second shell formed according to similar rules; hence, we call it Z16*vf*. One can wonder if other Friauf-polyhedron-based two-shell nanoclusters occur in intermetallics, in particular, with the second-shell atoms allocated above vertices and edges (16 + 42 = 58-atom shell, Z16*ve*) or above edges and faces (42 + 28 = 70-atom shell, Z16*ef*) of the Friauf polyhedron. Hence, these two nanoclusters can be treated in the same way as analogs of the Z12*ve* Mackay and Z12*ef* icosahedron-based two-shell clusters, respectively.

Table 4. Second Shells in Z15-Based Nanoclusters 1@15@*N* of D_{3h} Symmetry

number of atoms (*N*)	number of structures
41	1
44	1
47	20
50	10
53	156
54	1
56	5
59	1
71	36

In general, the problem can be formulated as follows: what are the typical ways of the growth of multishell nanoclusters based on different core polyhedra in intermetallics? We emphasize that the growth of metal clusters and nanoparticles of different sizes was modeled by various simulation methods,[5,6] but there were no investigations devoted to systematic search of particular multishell clusters in crystals. In this paper we study the occurrence of two-shell nanoclusters based on the Frank−Kasper polyhedra Z12 (icosahedron), Z14, Z15, and Z16 (Friauf polyhedron) and preserving the symmetry of the core polyhedra (Figure 1); we call them Frank−Kasper nanoclusters.

RESULTS AND DISCUSSION

Frank−Kasper Nanoclusters in Intermetallics. The parameters of the Frank−Kasper polyhedra (Figure 1) which are important for the subsequent discussion are given in Table 1. All faces of the polyhedra are triangular (they are also called

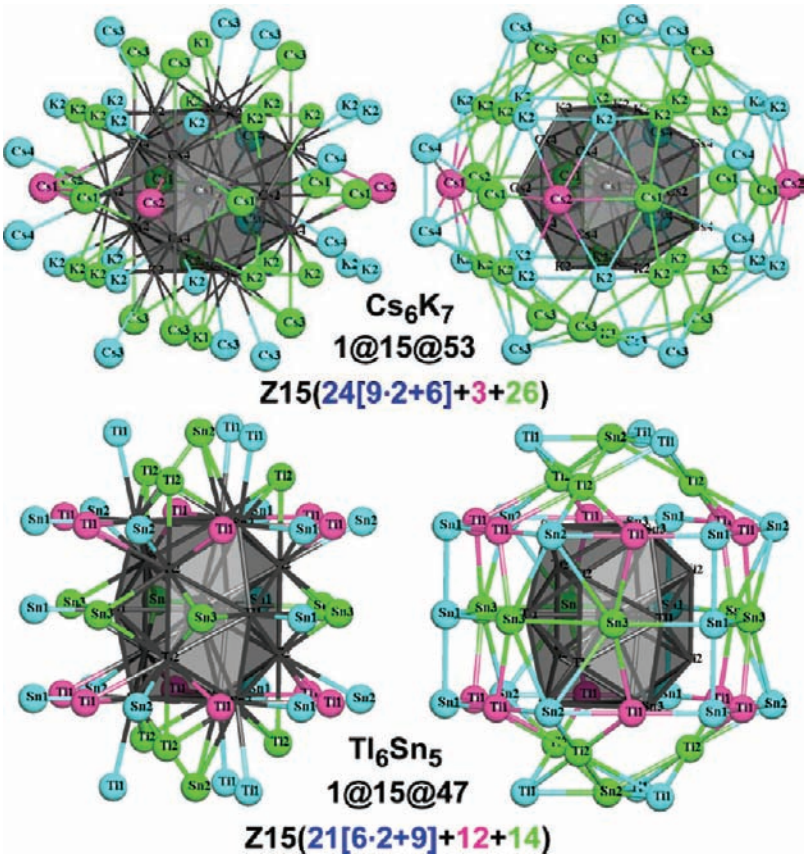

Figure 6. (Top) 1@15@53-atom nanocluster in the Cs_6K_7 crystal structure Z15 (24[9·2 + 6] + 3 + 26), and (bottom) 1@15@47-atom nanocluster in Ti_6Sn_5 crystal structure Z15(21[6·2 + 9] + 12 + 14). The symmetry of the nanoclusters is D_{3h}; the C_3 axis is vertical. The inner Z15 polyhedron is shown in black; the atoms of the outer shell which are connected to vertices, edges, or faces of the Z15 polyhedron are colored in cyan, magenta, or green, respectively.

dx.doi.org/10.1021/ic2005024 |*Inorg. Chem.* 2011, 50, 5714–5724

simplicial polyhedra), but only the icosahedron (Z12) is a *deltahedron* with all the faces as equilateral triangles.

The second shell will preserve the symmetry of the Frank−Kasper polyhedron if the atoms of the shell are projected to all vertices (v), edges (e), or faces (f) of the polyhedron, i.e., to obtain the most symmetric packing of atoms (corresponding to "magic" numbers) one of the four combinations ($v+f$, $v+e$, $e+f$, $v+e+f$) given in Table 1 should be realized.

To find the realizations of different kinds of second shells given in Table 1, we explored 22 951 crystal structures of intermetallics containing only metal atoms (no B, Si, or other metalloids) and stored in ICSD (release 2010/2)[17] and PCD (release 2009/10).[18] We extracted only the most symmetrical realizations of the nanoclusters with the point groups listed in Table 1. This is needed in order to unambiguously define the positions of atoms in the second shell as above vertices, faces, or edges. After knowing the topology (i.e., the connectivity) of the most symmetric (ideal) two-shell nanoclusters, we can search for any nanocluster with the same topology in geometrically distorted structures (see below monoclinic β-$Ta_{1.108}Al$ as an example). Since the maximum symmetry of Z12 (I_h) and Z14 (D_{6d}) is not compatible with translational symmetry, we searched within the maximal subgroups of I_h and D_{6d} for point symmetry compatible to crystal classes (in parentheses in Table 1).

Table 5. Second Shells in Z16-Based Nanoclusters 1@16@*N* of T_d Symmetry

number of atoms (N)	number of structures
30	1
40	4
44	20 (10[a])
46	9
48	7
50	3
52	1729
58	69 (64[b])
62	2
70	1

[a] Z16*vf* type. [b] Z16*ve* type.

Z12(Icosahedron)-Based Nanoclusters. The search for the most symmetrical shells sheathing the icosahedron core gave 10 different compositions from 32 to 62 atoms (Table 2). In most cases the "magic" numbers correspond to special types of nanoclusters: Bergman (Z12*vf*), Mackay (Z12*ve*), B, or Z12*ef*. The 50-atom shell was found in 2690 structures and is the most frequent in nanoclusters of both symmetries D_{3d} and T_h. While the D_{3d} symmetry of the 50-atom shell corresponds to nanocluster B Z12(24[6 + 6·3] + 6 + 20) (Figure 2), T_h symmetry describes a 63-atom nanocluster of quite another topology (Figure 4 left). It is a small distortion of the desired ideal nanocluster Z12*ef*, where all 50 atoms of the outer shell are

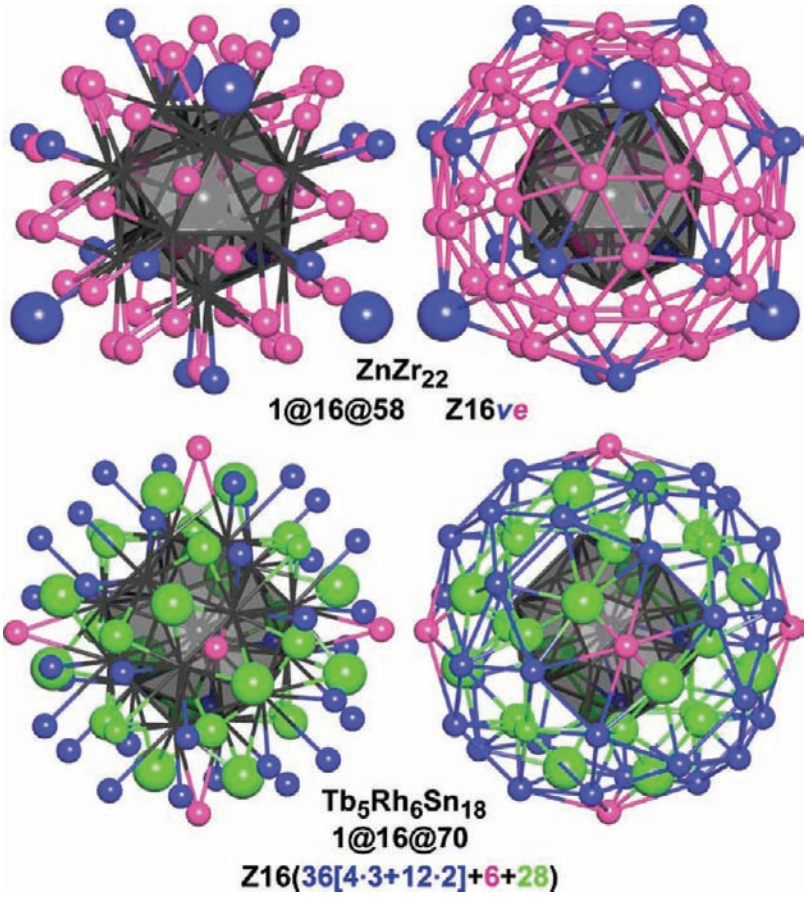

Figure 7. (Top) 1@16@58 nanocluster (Z16*ve*) in the $ZrZn_{22}$ crystal structure; (bottom) 1@16@70 nanocluster Z16 (36[4·3 + 12·2] + 6 + 28) in the $Tb_5Rh_6Sn_{18}$ crystal structure. The inner Z16 Friauf polyhedron is shown in black; the atoms of the outer shell which are connected to vertices, edges, or faces of the Friauf polyhedron are colored in blue, magenta, or green, respectively. The large balls correspond to the Zr, Tb, and Rh atoms.

dx.doi.org/10.1021/ic2005024 |*Inorg. Chem.* 2011, 50, 5714–5724

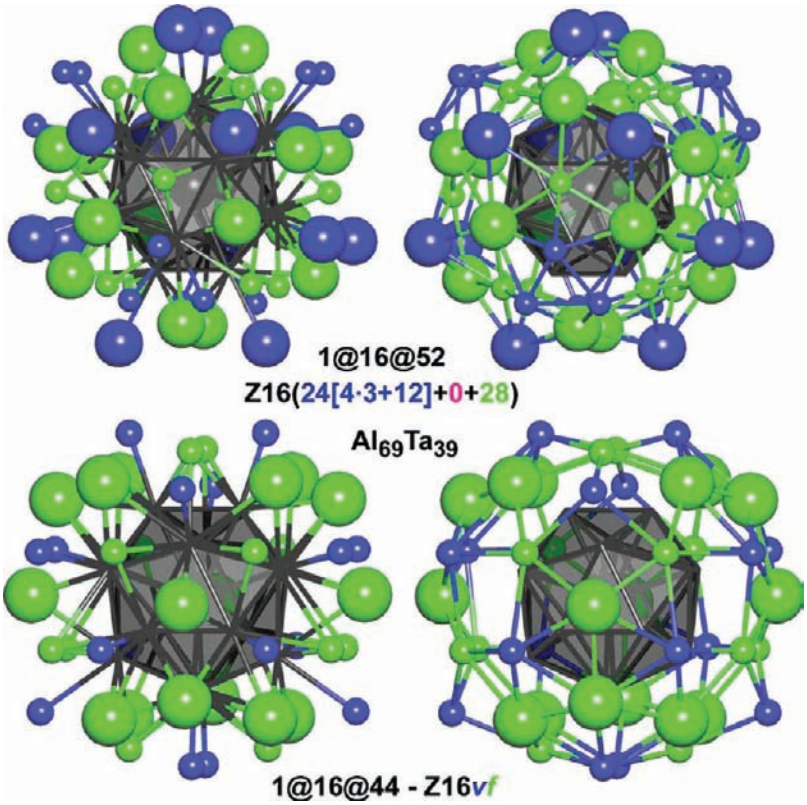

Figure 8. (Top) 1@16@52-atom Z16 (24[4·3 + 12] + 0 + 28) and (bottom) 1@16@44-atom Z16*vf* nanoclusters in the $Al_{69}Ta_{39}$ crystal structure. The inner Z16 Friauf polyhedron is shown in black; the atoms of the outer shell which are connected to vertices, centers of edges, or faces of the polyhedron are colored in blue, magenta, or green, respectively. The large balls correspond to the Ta atoms.

projected exactly to edges and faces of the inner icosahedron. The geometrical distortion moves 24 of the 30 "edge" atoms so they are no longer projected exactly to the middle of the edges of the inner icosahedron; in fact, the contact to one atom of the edge is much stronger than to the other (Figure 4). Thus, according to the topological criterion, these 24 atoms should have type "*v*" and the signature should be Z12(24[12·2] + 6 + 20), showing that it is a topological isomer of nanocluster B Z12(24[6·3 + 6] + 6 + 20), the difference being only in the distribution of the bonds of the 24 "*v*" atoms. Nonetheless, we will use the name Z12*ef* for the Z12(24[12·2] + 6 + 20) cluster keeping in mind that the projections of all 24 "*v*" atoms fall over the edges not vertices of the icosahedron. All 374 structures containing Z12*ef* belong to the structure types β-W and Cr_3Si. Note that in these structures the Z12*ef* nanoclusters interpenetrate to each other. Another abundant type of nanocluster is the one with 44 atoms in the outer shell observed in 143 structures, and it has a distorted Mackay shell with two additional atoms. The Bergman-like 32-atom and Mackay-like 42-atom shells are also among the most frequently observed ones. The role of the Bergman Z12*vf*, Mackay Z12*ve*, and Z12*ef* nanoclusters in assembling intermetallic structures will be discussed in detail below.

In Table 2 we give data for nanoclusters that have an atom in the center. As the noncentered icosahedral atomic configuration is also stable in intermetallics, all of the main types of nanoclusters (Z12*vf*, Z12*ve*, Z12*ef*) can exist noncentered. However, this is typical only for the Bergman-type (Z12*vf*) configurations: we found 82 structures containing "empty" Bergman clusters. Other types of noncentered nanoclusters are occasional (see Supporting Information).

Z14-Based Nanoclusters. As for the icosahedron, there are two possible maximal symmetries of the Z14 polyhedron, D_{3d} and C_{6v}; however, the first one is not realized in intermetallics. Instead, we found many examples of the maximal D_{3d} subgroup, D_3 (Table 3). Only one of the combinations reported in Table 1 has been found: the number 50 that formally corresponds to the outer-shell atoms allocated above vertices (14) and edges (36) of the inner Z14 polyhedron: Z14*ve*. However, the real $(v + e + f)$ motifs observed in both symmetries are quite another. In C_{6v} $(v + e + f)$ is (26[1·7 + 6·2 + 7] + 0 + 24), i.e., only all 24 faces are centered in the projection by atoms of the second shell, while the other 26 out of 50 atoms occupy the positions above vertices. The edges of the core Z14 polyhedron are not centered according to the topological criterion, although 18 atoms of the second shell are projected to edges (but not to the center of the edge). All structures of this kind belong to closely related structure types $ScNi_6Ge_6$ and $LiFe_6Ge_6$. The second shell is nonspherical (Figure 5 top) due to the occurrence of atoms of quite different sizes, which explains the unusual $(v + e + f)$ arrangement. In the case of D_3 symmetry (structure types Ti_5Ga_4 and Hf_5CuSn_3), the $(v + e + f)$ symbol (20[6·3 + 2] + 18 + 12) is more ambiguous: not all 14 vertices, 36 edges, or 24 faces of the core Z14 polyhedron correspond to the atoms of the second shell. The same concerns the most abundant type (270 cases) of the second shell: the 47-atom shell with D_3 symmetry has the $(v + e + f)$ signature (20[6·3 + 2] + 9 + 18). It occurs in the Mn_5Si_3 and $Zr_3Ti_2Ga_3$ structure types closely related to the Ti_5Ga_4 and

dx.doi.org/10.1021/ic2005024 |*Inorg. Chem.* 2011, 50, 5714–5724

Hf_5CuSn_3 structure types. The other abundant type (146 cases) of the 56-atom shell of the C_{6v} symmetry exists in three quite similar structure types ($TiBe_{12}$, $MgFe_6Ge_6$, and $Mn_4Fe_3Ge_6$). The arrangement of atoms in the second shell of the nanocluster is quite similar to the 50-atom-type shell but has six additional atoms above the edges of the Z14 polyhedron: $(v + e + f) = (26[1\cdot7 + 6\cdot2 + 7] + 6 + 24)$ (Figure 5, bottom).

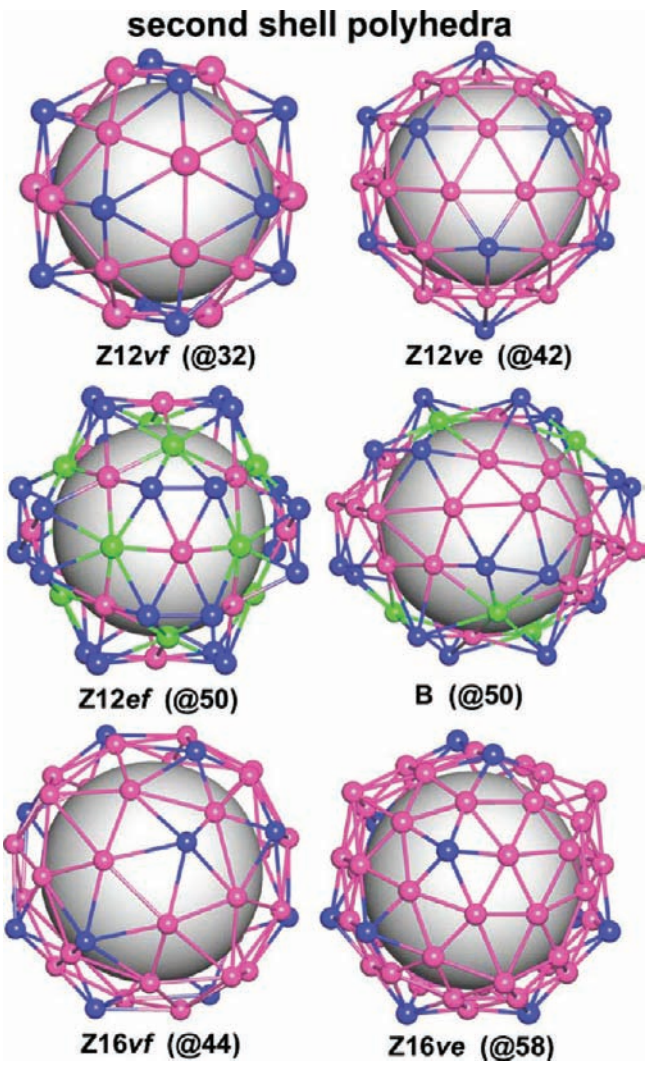

Figure 9. Second shells of Bergman (32 vertices), Mackay (42 vertices), Z12*ef*, B (both of 50 vertices), Z16*vf* (44 vertices), and Z16*ve* (58 vertices) nanoclusters. Five-, six-, and seven-coordinated vertices are colored in blue, magenta, and green, respectively.

Z15-Based Nanoclusters. As for the Z14-based nanoclusters, the numbers of atoms in the second shell of the Z15-based nanoclusters (Table 1) corresponding to ideal $(v + e + f)$ signatures are very rare (41, 54 bold numbers in Table 4). In the most typical 53-atom shell the atoms are allocated according to the scheme $(24[9\cdot2 + 6] + 3 + 26)$ (Figure 6, top for Cs_6K_7),[19] i.e., like in the Z14-based nanoclusters they prefer to occupy the positions above the centers of faces of the inner polyhedron. Less regular is the 47-atom shell in the Ti_6Sn_5 crystal structure[20] with the $(v + e + f)$ distribution $(21[6\cdot2 + 9] + 12 + 14)$ (Figure 6, bottom). Other types of shells are rarer (Table 4) and have irregular $(v + e + f)$ symbols.

Z16 (Friauf)-Based Nanoclusters. This type of nanocluster demonstrates the same diversity of the second shells as the icosahedron-based nanoclusters: they have 10 different compositions (Table 5). As mentioned above, the 44-atom shell with $(v + e + f) = (16 + 0 + 28)$ was found in the A nanocluster in β-Mg_2Al_3 (Figure 3). The next "magic" number (58) gives us one more fascinating nanocluster that has the most regular form in the $ZrZn_{22}$ structure type: the atoms of the second shell occupy the positions right above the vertices and edges of the core Friauf polyhedron, $(v + e + f) = (16 + 42 + 0)$ (Figure 7, top). Thus, while the A nanocluster (Z16*vf*) can be considered as a Friauf-based analog of the Bergman cluster, this Z16*ve* nanocluster resembles the Mackay cluster. The resemblance even increases if one draws attention to all atoms of the first shell, and almost all atoms of the second shell are equal in size (Zn atoms).

The "magic" number 70 $(v + e + f) = (0 + 42 + 28)$ occurs only in $Tb_5Rh_6Sn_{18}$,[21] where the second shell is essentially distorted due to low coordination of tin atoms, and according to the topological criterion the signature is $(36[4\cdot3 + 12\cdot2] + 6 + 28)$ (Figure 7, bottom). The smallest number (30) is realized also in a tin-containing nanocluster in the Ba—Na—Sn intermetallics[22] due to the same reason, since in this case the Friauf-like shell is composed only by tin atoms; this structure can be considered as a Zintl phase and can hardly be described in a cluster approach.

The most abundant type of the second shell containing 52 atoms, which can be seen in a Ta—Al phase, $Al_{69}Ta_{39}$ (Figure 8, top),[23] has $(v + e + f) = (24[4\cdot3 + 12] + 0 + 28)$. All faces of the Friauf polyhedron are centered in a projection by the atoms of the second shell; there are triples of Al atoms that are projected to edges of the Friauf polyhedron but topologically have type "*v*" (they are connected to the same vertex of the Friauf polyhedron, Figure 8, top). In this structure there is also a nanocluster of the

Table 6. Occurrence of the Second Shells of Some Types of Nanoclusters with Non-Frank—Kasper Polyhedral Cores

			number of *n*-coordinated atoms				
Frank—Kasper nanocluster	maximal crystallographic symmetry	number of atoms in the second shell	*n* = 5	*n* = 6	*n* = 7	non-Frank—Kasper cores	number of structures
Z12*vf* (Bergman)	T_h	32	12	20	0	dodecahedron	231 (D20*vf*)
Z12*ve* (Mackay)	T_h	42	12	30	0	cube, dodecahedron[a]	2, 12 (D20*ef*)
Z12*ef*	T_h	50	24	14	12	dodecahedron[a]	12
B	D_{3d}	50	18	26	6		
Z16*vf*	T_d	44	12	32	0		
Z16*ve*	T_d	58	12	46	0		

[a] See text for details of the relation between the dodecahedral core, the Mackay-type, and the Z12*ef*-type shells.

dx.doi.org/10.1021/ic2005024 |*Inorg. Chem.* 2011, 50, 5714–5724

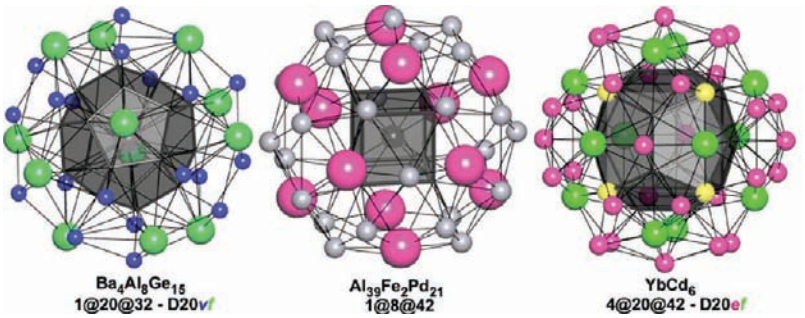

Figure 10. (Left) Bergman-type 32-atom shell sheathing a dodecahedral core in $Ba_4Al_8Ge_{15}$ and the resulting D20*vf* nanocluster. Ba atoms projecting to the dodecahedron faces are green; Al and Ge atoms projecting to the dodecahedron vertices are blue. (Middle) Mackay-type 42-atom shell sheathing a cubic core in $Al_{39}Fe_2Pd_{21}$. Pd and Al atoms are magenta and gray, respectively. (Right) Mackay-type 42-atom shell surrounding a dodecahedral core in $YbCd_6$. Cd and Yb atoms projecting to the dodecahedron edges and faces are magenta and green, respectively. Four out of eight dodecahedron vertices that together with the 42 atoms form a 50-atom Z12*ef* shell are shown as yellow balls. The internal tetrahedron is not shown.

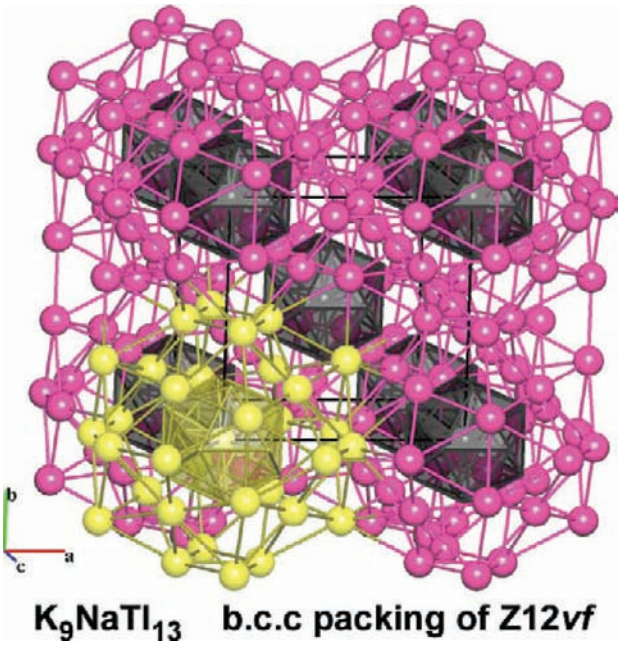

Figure 11. Body-centered cubic packing of the Bergman nanoclusters Tl@Tl12@Na2K30 in the K_9NaTl_{13} crystal structure.[33] The inner icosahedra are shown in black; one of the nanoclusters is selected in yellow.

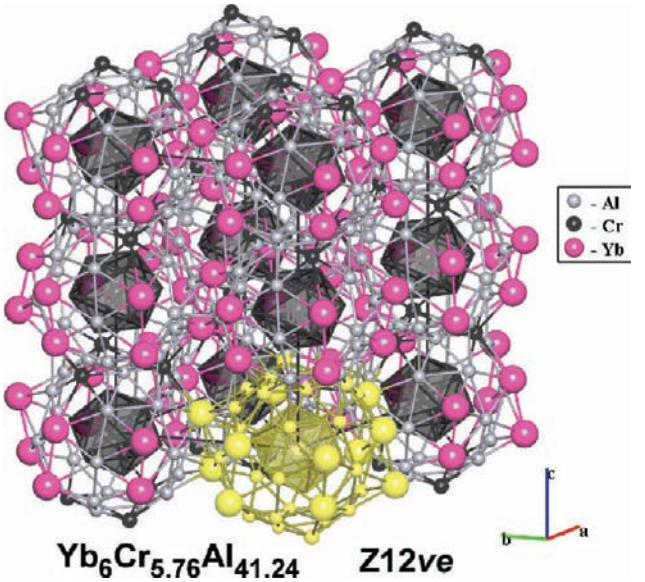

Figure 12. Hexagonal primitive packing of the Mackay nanoclusters Cr@Al12@Cr6Al24Yb12 in the $Yb_6Cr_{5.76}Al_{41.24}$ crystal structure.[34] The inner icosahedra are shown in black; one of the nanoclusters is selected in yellow. The Al@Al9Yb3 spacers are not shown.

Z16*vf* type based on another Friauf polyhedron (Figure 8, bottom), but the ratio Ta/Al in the second shell is different: 16/28 in Z16*vf* vs 28/24 for the 52-atom shell.

Outer Shells of Frank−Kasper Nanoclusters. The internal (core) Frank−Kasper polyhedra proved to be stable atomic configurations in the case of equal atoms or binary compounds.[14] Since the two-shell Frank−Kasper-based nanoclusters with a special $(v + e + f)$ signature are found in different intermetallic structure types, they can be considered stable as well. The question arises if the structure of the outer (second) shells is completely predetermined by the core polyhedra or the outer shells can be realized with different cores. To answer this question we looked separately for the second shells of the most abundant Bergman, Mackay, Z12*ef*, B, Z16*vf*, and Z16*ve* nanoclusters in our sample of 22 951 crystal structures of intermetallics. All shells are triangular facet and mostly composed of 5- and 6-coordinated vertices, except Z12*ef* and B that contain 7-coordinated vertices (Figure 9). As follows from Euler's theorem $(v - e + f = 2)$ applied to these polyhedra, the number of 5-coordinated vertices in such shells must be 12 more than the number of 7-coordinated ones (Table 6). Only the shells of maximal point symmetry (T_d, T_h, and D_{3d}) were considered; we ignored strongly distorted cases.

All Z12-based shells, except the second shell of the B nanocluster, were found to coexist together with other core polyhedra than icosahedron. The 32-atom Bergman shell sheathing pentagonal dodecahedron (D20) was revealed in 231 inorganic clathrates of the $Ba_4Al_8Ge_{15}$ structure type (Figure 10, left).[24] Since the atoms of the shell are projected to the vertices and centers of faces of the dodecahedron, the corresponding two-shell nanocluster can be called D20*vf*.

In $Al_{39}Fe_2Pd_{21}$,[25] the Mackay-like 42-atom shell is formed around a cube of Al atoms with an iron atom in the center that results in a Fe@Al8@Al30Pd12 nanocluster (Figure 10, middle).

dx.doi.org/10.1021/ic2005024 |*Inorg. Chem.* 2011, 50, 5714–5724

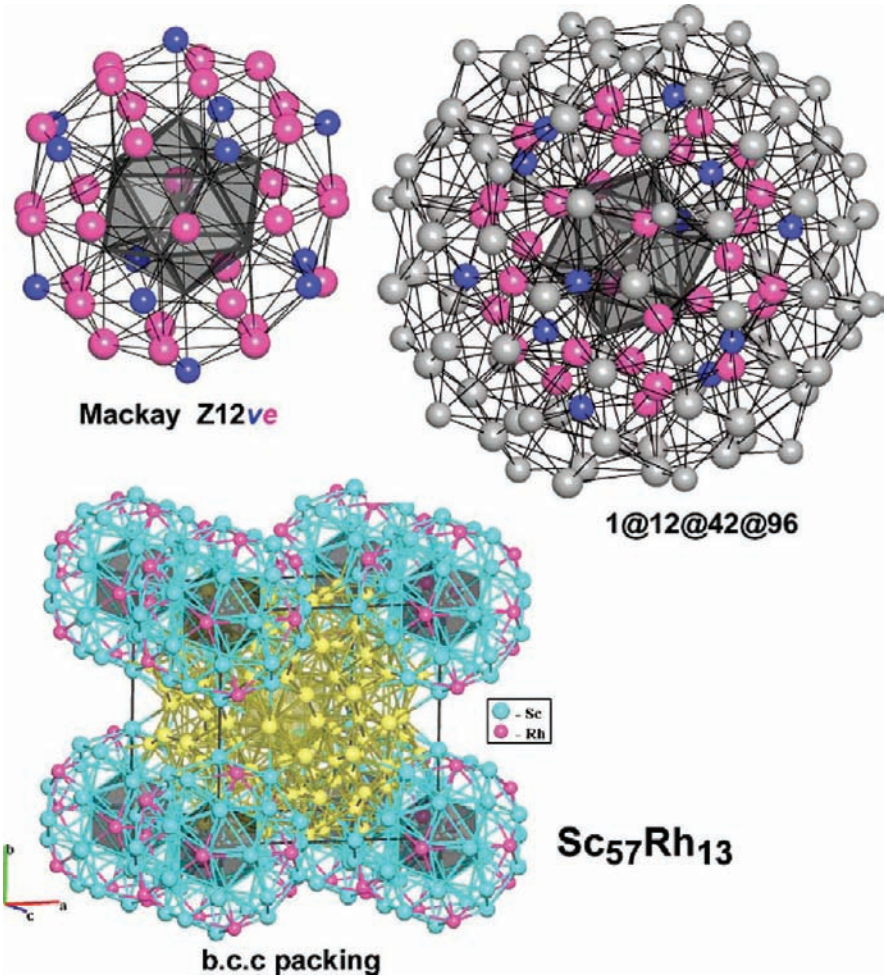

Figure 13. (Top) Two-shell (left) and three-shell (right) Mackay-like nanoclusters in the $Sc_{57}Rh_{13}$ crystal structure. The inner icosahedron is shown in black; the atoms of the second shell which are projected to vertices and centers of edges of the icosahedron are colored in blue and magenta, respectively; the atoms of the third shell are gray. (Bottom) Body-centered cubic packing of the nanoclusters; the three-shell nanocluster is selected in yellow.

A similar nanocluster Ag@Mg8@Mg30Ag12 occurs in the $Ag_{7.96}Mg_{25.04}$ phase;[26] no other examples with a cubic core were found.

In the quasicrystal-related structures belonging to YCd_6 and $YbCd_6$ structure types (12 representatives are known),[27−29] the outer 42-atom shell surrounds a pentagonal dodecahedron that is centered by a tetrahedron; the resulting nanoclusters (Figure 10, right) correspond to the Tsai clusters.[29] The 42-atom shell can be considered Mackay-like as its atoms are projected to all edges and faces of the inner dodecahedron; the corresponding nanocluster (without the tetrahedral core) can be assigned to the D20*ef* type. This example shows the relations between different types of shells and the possibility of their mutual transformation: if one includes eight Cd atoms of the dodecahedron into the second shell (these atoms are more distant from the center of the cluster than other 12 atoms), the resulting (42 + 8 = 50)-atom shell would be of the Z12*ef* type (Figure 10 right). The remaining 12 Cd atoms of the dodecahedron form a distorted icosahedron, so the Tsai cluster can be related to the Z12*ef* nanocluster of the β-W structure type. Besides the 12 structures just illustrated, no other examples of the Tsai/D20*ef* nanocluster were found.

The second shells of Friauf-based nanoclusters Z16*vf* and Z16*ve* were not revealed to fit other core polyhedra. At the same time, the systems of bonds between the core Friauf polyhedron and the outer shell were found different in different intermetallics; the graphs of the corresponding nanoclusters were nonisomorphic. This indicates that the two shells are not fixed in the nanoclusters and can slightly shift with respect to each other.

Assembling Intermetallic Structures with Frank−Kasper Nanoclusters. Recently,[16] we proposed a novel model of assembling intermetallic structures from nanoclusters, where the nanoclusters have no common internal atoms (do not interpenetrate) and include all nonequivalent atoms of the structure. If nanoclusters obey these conditions and, hence, build the whole structure, this can be considered as an additional argument for the existence of the nanoclusters in the melt. In particular, we showed[16] that the structures of $NaCd_2/\beta$-Mg_2Al_3 can be assembled with two types of two-shell Frank−Kasper nanoclusters, Z16*vf* and Z12(24[6 + 6·3] + 6 + 20) (the B cluster); moreover, the B cluster is preserved in the low-temperature phase β'-Mg_2Al_3.

Using TOPOS, we found three more two-shell Frank−Kasper nanoclusters that can assemble intermetallics in this way.

I. Z12vf (Bergman) Nanoclusters. The intermetallics of the K_9NaTl_{13}, $M_6Na_4Tl_{13}$ (M = K, Rb, Cs), and $K_8Na_3Tl_{13}$ structure types can be constructed with high-symmetrical (T_h) Bergman-type nanoclusters Tl@Tl12@Na2M30 and Tl@Tl12@Na8M24

dx.doi.org/10.1021/ic2005024 |*Inorg. Chem.* 2011, 50, 5714–5724

(M = K, Rb, Cs) or Tl@Tl12@Na6M26, respectively. The first two types of nanoclusters form a body-centered cubic (bcc) underlying net (that is the net constructed of the centers of nanoclusters)[30] (Figure 11), while the nanoclusters Tl@Tl12@Na6M26 are arranged in a face-centered cubic (fcc) underlying net. The Bergman-type nanoclusters Na@Hg12@Hg12K20 (T_h) and Li@In12@Li4In8Ca20 (D_{2h}) assemble crystal structures of $NaK_{29}Hg_{48}$[31] and $Ca_{18}Li_5In_{25.07}$[32] together with smaller one-shell polyhedra (spacers) K@Hg12K8 and Ca@Li11In2Ca4, respectively. Note that in all cases the authors of the original structure investigations do not mention the existence of the Bergman Z12*vf* clusters.

ii. Z12ve (Mackay) Nanoclusters. We have not found intermetallics that could be assembled only with Mackay-like nanoclusters. However, we found five structure types where these nanoclusters form the structure together with one more cluster.

In $Yb_6Cr_{5.76}Al_{41.24}$[34] the nanoclusters Cr@Al12@Cr6Al24Yb12 of D_{3d} symmetry (Figure 12, left) form a hexagonal primitive lattice (Figure 12 right), the voids of which are filled by one-shell icosahedron Al@Al9Yb3 spacers.

The same underlying net is observed in $La_4Mo_7Al_{51}$,[35] where the Mackay-like nanoclusters have the composition Mo@Al12@Mo6La6Al30 and the same symmetry. In both cases, the authors of the structural investigations do not talk about these clusters.

Almost undistorted (T_h) Mackay clusters Mo@Zn12@Zn30Mo12 were revealed in the $Mo_7Sn_{12}Zn_{40}$ crystal structure,[36] where they are separated by Zn_6 octahedra.

In the fascinating example $Sc_{57}Rh_{13}$[37] there are two types of almost ideal (T_h) Mackay-like clusters of the same composition Rh@Sc12@Sc30Rh12 (they were not noticed by the authors); the 12 Rh atoms of the second shell are projected to the vertices of the $RhSc_{12}$ icosahedron, while the 30 Sc atoms occupy the positions above the centers of edges (Figure 13, top left). However, when assembling the crystal structure, one of the nanoclusters acquires a third shell (Figure 13, top right) that contains 96 atoms; this number is a bit larger than the ideal number in the packing of equal balls (92). The resulting underlying net has the bcc topology (Figure 13, bottom).

In $Mg_{51}Zn_{20}$[38] and related $Ag_{17}Mg_{54}$[39] and $Hf_{54}Os_{17}$[40] the structure is composed of the Mackay nanoclusters packed in an fcc fashion with the tetrahedra Mg_4 or Hf_4 occupying the voids in the resulting framework.

iii. Z12ef Nanoclusters. In the recently studied β-$Ta_{1.108}Al$[41,42] the only building units are the Z12*ef* nanoclusters Al@Ta12@Ta16Al34 of a lower symmetry (C_i) but of the same form as Figure 4. As in β-W, the atoms of the second shell are shifted in the projection from the centers of edges of the inner icosahedron, but the topology of the nanocluster is preserved. The underlying net of β-$Ta_{1.108}Al$ has the fcc topology.[42]

In all these cases the first shell (inner icosahedron) is formed with atoms of the same kind. The second shell of the Bergman nanoclusters contains large atoms (alkali or alkaline earth), while the Mackay-like and Z12*ef* nanoclusters are composed with atoms of medium size of radius 1.2−1.5 Å. Insertion of large atoms (like Yb in $Yb_6Cr_{5.76}Al_{41.24}$) results in a distortion of the second shell (Figure 12). The Z14 and Z15 polyhedra do not play a significant role in assembling intermetallics; no nonintersecting multishell nanoclusters are formed with them for all structures from Tables 3 and 4.

CONCLUDING REMARKS

The Frank−Kasper nanoclusters considered in this paper show preferable local topological structures of intermetallic phases and possible ways of growth of nanoparticles, which can compose the entire crystal by assembling without mutual crossing. Unlike the nested-polyhedron models, the nanoclusters maintain the information on the crystal structure connectivity and can be unambiguously identified even in geometrically distorted motifs with computer methods. The second shells of the icosahedral nanoclusters can be realized with different core polyhedra and can shift around each other as rather independent objects. The computer-based nanocluster approach allows one to take into consideration the whole array of crystallographic information when studying forms, composition, and stability of nanoparticles. In contrast to simple theoretical models, like the model of packing of equal balls, the nanocluster approach can be applied to atomic systems of any composition. As opposed to simulation methods, the nanoclusters found with this formalism correspond to experimentally proved spatial configurations of atoms. These advantages of the nanocluster approach cause us to consider it as a promising new tool for comparative structural analysis of intermetallic phases (including quasicrystals) and nanoparticles.

ASSOCIATED CONTENT

Supporting Information. List of references to the crystal structures containing noncentered nanoclusters; full list of all the structures found/described are available upon request from the authors. This material is available free of charge via the Internet at http://pubs.acs.org.

AUTHOR INFORMATION

Corresponding Author

*Phone: +7-8463345445. Fax: +7-8463345417. E-mail: blatov@ssu.samara.ru.

ACKNOWLEDGMENT

V.A.B. is thankful for the 2009/2010 Fellowship from Cariplo Foundation & Landau Network-Centro Volta (Como, Italy) and partial funding from the MATHXPRE project of the University of Padova. V.A.B. and G.D.I. thank the Russian Foundation for Basic Research for grant no. 09-02-01269.

REFERENCES

(1) Mackay, A. L. *Acta Crystallogr.* **1962**, *15*, 1916.
(2) Bergman, G.; Waugh, J. L. T.; Pauling, L. *Acta Crystallogr.* **1957**, *10*, 254.
(3) Lord, E. A.; Mackay, A. L.; Ranganathan, S. *New Geometries for New Materials*; Cambridge University Press: Cambridge, 2006.
(4) Steurer, W.; Deloudi, S. *Acta Crystallogr.* **2008**, *A64*, 1.
(5) Ferrando, R.; Jellinek, J.; Johnston, R. L. *Chem. Rev.* **2008**, *108*, 845.Johnston, R. L. *Atomic and Molecular Clusters*; Taylor and Francis: London, 2002.
(6) Cambridge Cluster Database, http://www-wales.ch.cam.ac.uk/CCD.html.
(7) Steurer, W. *Philos. Mag.* **2006**, *86*, 1105.
(8) Ilyushin, G. D.; Blatov, V. A. *Acta Crystallogr.* **2009**, *B65*, 300.
(9) Blatov, V. A. *IUCr CompComm Newslett.* **2006**, *7*, 4.
(10) Samson, S. *Acta Crystallogr.* **1961**, *14*, 1229.
(11) Samson, S. *Nature* **1962**, *195*, 259.
(12) Samson, S. *Acta Crystallogr.* **1964**, *17*, 491.
(13) Samson, S. *Acta Crystallogr.* **1965**, *19*, 401.

(14) (a) Frank, F. C.; Kasper, J. S. *Acta Crystallogr.* **1958**, *11*, 184. (b) Delgado-Friedrichs, O.; O'Keeffe, M. *Acta Crystallogr.* **2010**, *A66*, 637.
(15) Shevchenko, V. Ya.; Blatov, V. A.; Ilyushin, G. D. *Struct. Chem.* **2009**, *20*, 975.
(16) Blatov, V. A.; Ilyushin, G. D.; Proserpio, D. M. *Inorg. Chem.* **2010**, *49*, 1811.
(17) Belsky, A.; Hellenbrandt, M.; Karen, V. L.; Luksch, P. *Acta Crystallogr.* **2002**, *B58*, 364http://www.fiz-karlsruhe.de/icsd_home.html.
(18) Villars, P.; Cenzual, K. *Pearson's Crystal Data-Crystal Structure Database for Inorganic Compounds (on CD-ROM)*; ASM International: Materials Park, OH, 2009.
(19) Simon, A.; Bramer, W.; Hillenkotter, B.; Kullman, H.-J. *Z. Anorg. Allg. Chem.* **1976**, *419*, 253.
(20) van Vucht, J. H. N.; Bruning, H. A. C. M.; Donkersloot, H. C.; de Mesquita, G. A. H. *Philips Res. Rep.* **1964**, *19*, 407.
(21) Vandenberg, J. M. *Mater. Res. Bull.* **1980**, *15*, 835.
(22) Bobev, S.; Sevov, S. C. *J. Am. Chem. Soc.* **2002**, *124*, 3359.
(23) Mahne, S.; Harbrecht, B. *J. Alloys Compd.* **1994**, *203*, 271.
(24) Eisenmann, B.; Schafer, H.; Zagler, R. *J. Less-Common Met.* **1986**, *118*, 43.
(25) Edler, F. J.; Gramlich, V.; Steurer, W. *J. Alloys Compd.* **1998**, *269*, 7.
(26) Kreiner, G.; Spiekermann, S. *Z. Anorg. Allg. Chem.* **2001**, *627*, 2460.
(27) Larson, A. C.; Cromer, D. T. *Acta Crystallogr.* **1971**, *B27*, 1875.
(28) Palenzona, A. *J. Less-Common Met.* **1971**, *25*, 367.
(29) Tsai, A. P.; Guo, J. Q.; Abe, E.; Takakura, H.; Sato, T. J. *Nature* **2000**, *408*, 537.
(30) Alexandrov, E. V.; Blatov, V. A.; Kochetkov, A. V.; Proserpio, D. M. *CrystEngComm*, **2011**, DOI: 10.1039/c0ce00636j.
(31) Deiseroth, H.-J.; Biehl, E. *J. Solid State Chem.* **1999**, *147*, 177.
(32) Mao, J.-G.; Goodey, J.; Guloy, A. M. *Inorg. Chem.* **2004**, *43*, 282.
(33) Cordier, G.; Muller, V. *Z. Naturforsch. B* **1994**, *49*, 935.
(34) Yanson, T. I.; Manyako, M. B.; Bodak, O. I.; Zarechnyuk, O. S.; Gladyshevskii, R. E.; Cerny, R.; Yvon, K. *Acta Crystallogr.* **1994**, *50*, 1529.
(35) Thiede, V. M. T.; Jeitschko, W. *J. Solid State Chem.* **1999**, *143*, 198.
(36) Hillebrecht, H.; Kuntze, V.; Gebhardt, K. *Z. Kristallogr.* **1997**, *212*, 840.
(37) Cenzual, K.; Chabot, B.; Parthé, E. *Acta Crystallogr.* **1985**, *C41*, 313.
(38) Higashi, I.; Shiotani, N.; Uda, M.; Mizoguchi, T.; Katoh, H. *J. Solid State Chem.* **1981**, *36*, 225.
(39) Arakcheeva, A. V.; Karpinskii, O. G.; Kolesnichenko, V. E. *Sov. Phys. Crystallogr.* **1988**, *33*, 907.
(40) Cenzual, K.; Chabot, B.; Parthe, E. *Acta Crystallogr.* **1985**, *C41*, 313.
(41) Boulineau, A.; Joubert, J. M.; Cerny, R. *J. Solid State Chem.* **2006**, *179*, 3385.
(42) Conrad, M.; Harbrecht, B. *Phil. Mag. Lett.* **2007**, *87*, 493.